Check for updates

The synthesis of polyisoxazoles incorporating fatty acids†

Andrew James Clark, [ID] * Nyle Owen Saul Jones and Abdulrahman Alhathir [ID]

Polyisoxazoles derived from thermal and base-mediated nitrile-*N*-oxide cycloaddition to fatty amide derived alkynes with up to 44% biobased content are described and their structural and thermal properties reported. Glass transition temperatures, T_g, (ranged from −1.1 °C to 62.0 °C), and measured molecular weights were dependent upon the level of unsaturation in the fatty amide feedstock, the regiochemistry of the dinitrile-*N*-oxide monomer and whether polymerisation was thermally or base-mediated. For base-mediated processes the solvent played a critical role in controlling the molecular weights of the obtained polymers. MALDI-TOF-MS, infrared and ^{1}H and ^{13}C NMR analysis indicated polymerisation proceeds to give mixtures of linear, cyclic, branched or furoxan incorporated materials.

Introduction

Polytriazole synthesis *via* click reactions of suitably functionalised azides and alkynes is well documented.[1,2] The analogous cycloaddition reactions between alkynes (**A**, Fig. 1) and suitably functionalized nitrile-*N*-oxides (**B**, Fig. 1) have received less attention.[3] The uncatalyzed thermal cycloaddition of nitrile-*N*-oxides with alkynes normally proceeds with high regioselectivity for 3,5-isoxazoles.[4] Early work on nitrile-*N*-oxide cycloaddition polymers was carried out in the 1960's and 1970's.[5–7] More recently, Takata *et al.* have demonstrated a thermal, metal free, mild and high yielding approach to give both polyisoxazoles and polyisoxazolines from hydroximoyl chlorides **1a** and **1b** and conventional petrochemical based diyne monomers.[8–10] Post polymerisation reductive modification of polyisoxazoles allows access to poly-β-aminoalcohols and poly-β-enaminoketones with interesting properties.[9] However, the application of this approach toward biobased polymers is less developed. In 2023, a base-mediated thermal cycloaddition of vanillin derived nitrile-*N*-oxides to alkenes to give the related polyisoxazolines was described (71% biobased).[11] In the study a range of biobased polyisoxazoline materials were prepared and used in encapsulating a thermoelectric generator with glass transition temperature ranging between 60–80 °C. The analysis and formation of polyisoxazoline derivatives however is complicated by the formation of diastereomers in

each propagation event. Thermal self-dimerization of nitrile-*N*-oxides to give furoxans **2**,[12] can also complicate polymerisations and lead to lower molecular weights by removing desired reactive nitrile-*N*-oxide functional groups thus altering the stoichiometry of the reacting functional groups.

The use of vegetable oils and fatty acid derivatives to produce biobased materials is well established.[13,14] While vegetable oil based polytriazoles, derived from azide–alkyne click reactions have been reported,[15–17] the corresponding nitrile-*N*-oxide 'click' chemistry of fatty acid derivatives has not been explored. In principle, polyisoxazoles derived from fatty acid derivatives, should present with relatively low T_g's, complementing those prepared from vanillin.[11] Incorporation of fatty acid derivatives derived from palmitic (16 : 0), stearic
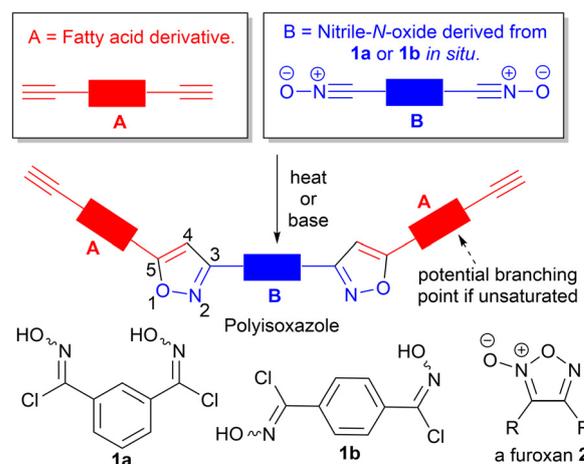
Chemistry Department, The University of Warwick, Coventry, CV4 7AL, UK.
E-mail: A.J.Clark@warwick.ac.uk

†Electronic supplementary information (ESI) available: Additional ^{1}H, ^{13}C, COSY, HMBC and HMQC spectra and variable temperature NMR spectra, infrared spectra, MALDI-TOF-MS, SEC traces and TGA, DSC and DMA thermogram data. See DOI: https://doi.org/10.1039/d4py00102h

Fig. 1 General approach to the synthesis of fatty acid derived polyisoxazoles.

Polymer Chemistry

(18:0), oleic (18:1), linoleic (18:2) and linolenic (18:3) acids should allow fine-tuning of polymer properties with unsaturated fatty acid derivatives potentially providing additional cross-linking opportunities *via* competing isoxazoline formation from their internal alkene groups, Fig. 1. To determine the value of such materials we undertook exploratory work to incorporate a range of different fatty acid derivatives into polyisoxazoles and report the effect on the molecular weight and thermal properties of the polymers produced.

In this study we show that the thermal properties of the fatty amide derived polyisoxazole materials are dependent upon the method of polymerisation, the regiochemistry of the nitrile-*N*-oxide precursor and the feedstock utilised, and that glass transition temperatures complement those reported for vanillin derived polymers. We use MALDI-TOF-MS to identify the types of species present in the new materials and show that depending upon the reaction conditions used, linear, cyclic, or furoxan incorporated materials can be detected. Attempts to limit competing furoxan formation by conducting the polymerisations at room temperature using base-mediated approaches in the renewable solvent EtOH are described. We also prepared a range of uniform oligomers to provide reference samples for GPC analysis and undertake variable temperature ^{1}H NMR studies to understand barriers to rotation in the oligomers and by extrapolation the polymers.

Experimental

Material

All chemicals and solvents were purchased from Sigma Aldrich and used as received unless otherwise stated. Compounds **1a**,[8] **1b**,[8] **2** (R = Ph),[18] and **4a–4f**,[19,20] were prepared according to literature procedures.

Characterization

Nuclear magnetic resonance (NMR). ^{1}H and ^{13}C NMR spectra were recorded with Bruker Avance AM 400 and 500 MHz spectrometers. Chemical shifts are given in parts per million (ppm) relative to CHCl$_3$, ^{1}H δ = 7.26 ppm and δ = ^{13}C 77.16 ppm. VT-NMR experiments used either d$_6$-DMSO or d$_8$-toluene.

Infrared. IR spectra were performed on a Bruker ALPHA platinum ATR Fourier transform spectrometer. Absorptions are given in wavenumbers (cm^{-1}).

Size exclusion chromatography (SEC). The solvents CHCl$_3$, DMF or THF were used as eluent. When CHCl$_3$ or DMF were used as eluent an Agilent Infinity II MDS instrument equipped with differential refractive index (DRI), viscometry (VS), dual angle light scatter (LS) and multiple wavelength UV detectors was used. The system was equipped with 2× PLgel Mixed C columns (300 × 7.5 mm) and a PLgel 5 µm guard column. When the eluent was CHCl$_3$, 2% triethylamine was used as an additive and samples were run at 1 mL min^{-1} at 30 °C. With DMF as eluent, 5 mmol NH$_4$BF$_4$ was the additive. Samples were run at 1 mL min^{-1} at 50 °C. When THF was used as eluent an Agilent 390-MDS with autosampler using a PLgel

5.0 µm bead-size guard column (50 × 7.5 mm), followed by two linear 5.0 µm bead-size PLgel Mixed D columns (300 × 7.5 mm) and a differential refractive index detector was used, and samples were run at 1 mL min^{-1} at 30 °C. PMMA and polystyrene standards were used for calibration.

Differential scanning calorimetry (DSC), thermal gravimetric analysis (TGA) and dynamic mechanical analysis (DMA). DSC was achieved using a Mettler-Toledo DSC1 or a TA Discovery DSC 2500 with autosampler. DSC samples were all heated and cooled under N$_2$ in 40 µl aluminium pans, specific heating cycles are described in the ESI.† The glass transition temperature (T_g) and the melting point (T_m) were obtained from the second heating cycle. TGA was achieved using a Mettler-Toledo TGA or a TA Instruments Discovery SDT 650 with autosampler. TGA samples, under nitrogen, were heated from 25–600 °C at 10 °C min^{-1} in 40 µl aluminium pans unless stated otherwise. DMA was run using a PerkinElmer DMA 8000 with liquid nitrogen cooling. Samples were loaded in aluminium envelopes and analysed using the single cantilever method between −60 °C to 250 °C at a heating rate of 5 °C min^{-1}. The frequency of the applied oscillating force was set at 1 Hz.

Matrix assisted laser desorption ionisation – time of flight mass spectroscopy (MALDI-TOF-MS). Spectra were obtained using a Bruker Autoflex Speed MALDI-TOF. Samples were either prepared: (i) using DMF doped with NaI (0.1 mg mL^{-1}) and the matrix (DCTB) (40 mg mL^{-1}) spotted on a ground steel plate and dried in a vacuum oven at 25 °C and 0.01 atm for 30 min; or (ii) by dissolving 2 mg of polymer mixed with 0.1 mg of NaI in 1 mL of THF. The MALDI matrix was prepared by dissolving DCTB (20 mg) in THF (1 mL). Equal volumes (5 µl) of the two solutions were mixed and 5 µl of the mixture was spotted on the MALDI-TOF plate. All samples were measured in reflectron mode and spectra were calibrated against a 3000–8000 g mol^{-1} PEG poly(ethylene glycol) standard.

Monomer synthesis

***N,N*-Di(prop-2-yn-1-yl)acetamide 3.** Dipropargyl amine (1.0 g, 10.7 mmol, 1.0 eq.) was added dropwise to acetic anhydride (1.3 g, 12.9 mmol, 1.2 eq.) under nitrogen at 0 °C. After addition was complete the temperature was increased to 100 °C for 1 hour. The mixture was quenched with water (30 mL) and extracted with CHCl$_3$ (3 × 25 mL). The organic extracts were dried over MgSO$_4$, and the solvent was removed *in vacuo* to leave a crude dark brown liquid, which was purified through a silica plug (R_f = 0.3, 1:1 EtOAc:40–60° pet. ether) to give **3** as a pale-yellow liquid (1.4 g, 93%); ν_{max}/cm^{-1}: 3290 (≡C–H), 3245 (≡C–H), 2978 (C–H), 2119 (C≡C), 1646 (C=O), 1413 (C–N); ^{1}H NMR (500 MHz, CDCl$_3$) δ 4.31 (d, J = 2.0 Hz, 2H, CH$_2$), 4.18 (d, J = 2.0 Hz, 2H, CH$_2$), 2.30 (t, J = 2.0 Hz, 1H, CH), 2.22 (t, J = 2.0 Hz, 1H, CH), 2.18 (s, 3H, CH$_3$); ^{13}C NMR (126 MHz, CDCl$_3$) δ 170.06 (C=O), 78.49 (C≡$\underline{C}$H), 77.79 (C≡$\underline{C}$H), 73.09 ($\underline{C}$≡CH), 72.40 ($\underline{C}$≡CH), 37.08 (CH$_2$), 33.90 (CH$_2$), 21.58 (CH$_3$); m/z (ES$^+$) calcd (C$_8$H$_9$NO + Na$^+$): 158.0576, found: 158.0577 (M + Na$^+$).

General procedure for 5a–f, (Fig. 2). Part 1: *N*-Methyl morpholine (1.1 eq.) was added to the appropriate fatty acid (1 eq.,
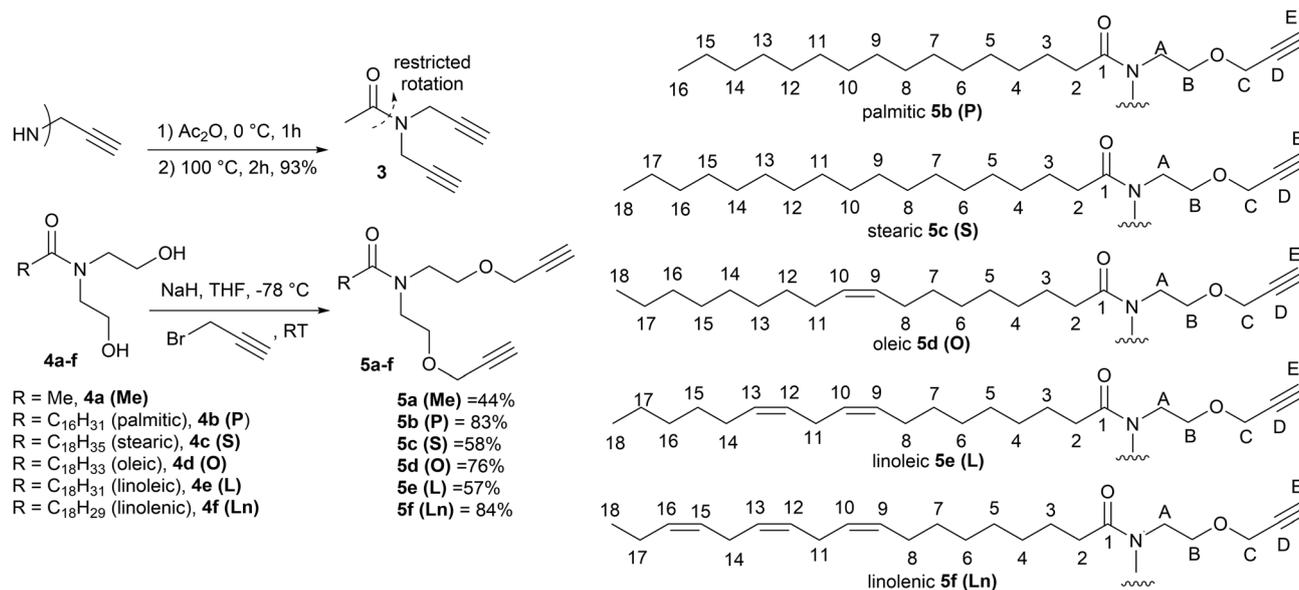
Fig. 2 Synthetic route to the monomers used in this study, (**3** and **5a–f**) and the numbering system used in the NMR assignments in the Experimental section.

0.5 M) in dry Et₂O for saturated fatty acids or dry THF for unsaturated fatty acids. Ethyl chloroformate (1.1 eq.) was added dropwise and the reaction was stirred for 30 minutes. The precipitate was removed by filtration and the filtrate was added dropwise to diethanolamine (1.1 eq., 0.5 M) and triethylamine (1.1 eq., 0.5 M) in dry DMF at room temperature under N₂. After 3 h the reaction was quenched with 2 M HCl (20 mL) and extracted with Et₂O (200 mL).

The organic layer washed with water (2 × 50 mL) and brine (50 mL), before drying over MgSO₄. The solvent was removed *in vacuo* to leave a crude product. Unsaturated amides **4d–f** were purified by column chromatography through a silica plug (EtOAc, R_f = 0.2). Saturated amides **4b–c** were purified by recrystallisation from Et₂O. Part 2: The amides **4b–f** from part 1 and **4a**[18] (1 eq., 0.5 M in dry THF) were added to NaH (60% in mineral oil, 2.2 eq.) under N₂. [For unsaturated compounds the reactions were carried out at −78 °C, saturated compounds were reacted at 0 °C.] After 30 min propargyl bromide (80 wt% in toluene, 2.2 eq.) was added dropwise and the reaction mixture was left to warm to room temperature overnight. Water (10 mL) was added dropwise followed by 2 M HCl (10 mL). The solvent was removed *in vacuo* and the residue was taken into Et₂O (150 mL) and washed with water (2 × 50 mL) and brine (50 mL) before drying over MgSO₄. After removal of the solvent *in vacuo* the products **5a–f** were purified through a silica plug (1 : 4 EtOAc : 40–60° pet. ether).

***N,N*-Bis(2-(prop-2-yn-1-yloxy)ethyl)acetamide 5a(Me).** Part 2: **4a** (7.08 g, 48.1 mmol), NaH (60% in mineral oil, 4.24 g, 105.9 mmol), and propargyl bromide (80% in toluene, 15.75 g, 105.9 mmol). Pale yellow oil (4.72 g, 44%); R_f = 0.3, 16 : 1 EtOAc : 40–60° pet. ether; ν_{max}/cm^{-1}: 3283 (C≡C–H), 2941 (C–H), 2869 (C–H), 2114 (C≡C), 1625 (C=O), 1419 (C–N), 1098 (C–O); ¹H NMR (500 MHz, CDCl₃) δ 4.10 (d, J = 2.5 Hz,

2H, Hᶜ), 4.08 (d, J = 2.5 Hz, 2H, Hᶜ), 3.66–3.58 (m, 4H, Hᴮ), 3.58–3.47 (m, 4H, Hᴬ), 2.42 (t, J = 2.5 Hz, 1H, Hᴱ), 2.39 (t, J = 2.5 Hz, 1H, Hᴱ), 2.08 (s, 3H, CH₃); ¹³C NMR (126 MHz, CDCl₃) δ 171.33 (C=O), 79.63 (Cᴰ), 79.32 (Cᴰ), 74.88 (Cᴱ), 74.56 (Cᴱ), 68.65 (Cᴮ), 67.88 (Cᴮ), 58.49 (Cᶜ), 58.29 (Cᶜ), 49.70 (Cᴬ), 46.16 (Cᴬ), 21.79 (CH₃); m/z: (ES⁺) calcd (C₁₂H₁₇NO₃ + Na⁺): 246.1101, found: 246.1102 (M + Na⁺).

***N,N*-Bis(2-(prop-2-yn-1-yloxy)ethyl)palmitamide 5b(P).** Part 2: **4b** (9.4 g, 27.3 mmol), NaH (60% in mineral oil 2.4 g, 60.2 mmol), propargyl bromide (80% in toluene, 9.0 g, 60.2 mmol). White solid (9.5 g, 83%); R_f = 0.3, 1 : 4 EtOAc : 40–60° pet. ether; m.p. 38–40 °C; ν_{max}/cm^{-1} 3306 (≡C–H), 2916 (C–H), 2849 (C–H), 2114 (C≡C), 1611 (C=O); 1466 (C–H), 1412 (C–N), 1098 (C–O), 1037 (C–O); ¹H NMR (500 MHz, CDCl₃) δ 4.14 (d, J = 2.0 Hz, 2H, Hᶜ), 4.12 (d, J = 2.0 Hz, 2H, Hᶜ), 3.70–3.62 (m, 4H, Hᴮ), 3.62–3.54 (m, 4H, Hᴬ), 2.43 (t, J = 2.0 Hz, 1H, Hᴱ), 2.41 (t, J = 2.0 Hz, 1H, Hᴱ), 2.38–2.33 (t, J = 7.5 Hz, 2H, H²), 1.70–1.57 (m, 2H, H³), 1.36–1.21 (m, 24H, H⁴⁻¹⁵), 0.87 (t, J = 7.0 Hz, 3H, H¹⁶); ¹³C NMR (126 MHz, CDCl₃) δ 173.94 (C=O), 79.80 (Cᴰ), 79.45 (Cᴰ), 74.90 (Cᴱ), 74.54 (Cᴱ), 68.87 (Cᴮ), 68.17 (Cᴮ), 58.63 (Cᶜ), 58.41 (Cᶜ), 48.91 (Cᴬ), 46.52 (Cᴬ), 33.25 (C²), 32.06 (C¹⁴), 29.91–29.40 (Cᶜʰᵃⁱⁿ), 25.47 (C³), 22.83 (C¹⁵), 14.27 (C¹⁶); m/z: (ES⁺) calcd (C₂₆H₄₅NO₃ + Na⁺): 442.3292, found: 442.3283 (M + Na⁺).

***N,N*-Bis(2-(prop-2-yn-1-yloxy)ethyl)stearamide 5c(S).** Part 2: **4c** (13.0 g, 35.0 mmol), NaH (60% in mineral oil, 3.1 g), and propargyl bromide (80% in toluene, 11.5 g). White solid (9.1 g, 58%); R_f = 0.3, 1 : 4 EtOAc : 40–60° pet. ether; m.p. 41–43 °C; ν_{max}/cm^{-1} 3307 (≡C–H), 2915 (C–H), 2848 (C–H), 2114 (C≡C), 1612 (C=O), 1466 (C–H), 1414 (C–N), 1099 (C–O), 1037 (C–O); ¹H NMR (500 MHz, CDCl₃) δ 4.15 (d, J = 2.0 Hz, 2H, Hᶜ), 4.12 (d, J = 2.0 Hz, 2H, Hᶜ), 3.67 (t, J = 5.0 Hz, 2H, Hᴮ), 3.64 (t, J = 5.0 Hz, 2H, Hᴮ), 3.61–3.57 (m, 4H, Hᴬ), 2.43 (t, J = 2.0 Hz, 1H,

H^E), 2.41 (t, J = 2.0 Hz, 1H, H^E), 2.36 (t, J = 7.5 Hz 2H, H^2), 1.65–1.59 (m, 2H, H^3), 1.32–1.24 (m, 28H, H^{4-17}), 0.88 (t, J = 7.0 Hz, 3H, H^{18}); ^{13}C NMR (126 MHz, CDCl$_3$) δ 173.93 (C=O), 79.81 (C^D), 79.45 (C^D), 74.90 (C^E), 74.54 (C^E), 68.88 (C^B), 68.18 (C^B), 58.63 (C^C), 58.41 (C^C), 48.91 (C^A), 46.52 (C^A), 33.25 (C^2), 32.07 (C^{16}), 29.93–29.40 (C^{chain}), 25.47 (C^3), 22.84 (C^{17}), 14.27 (C^{18}); m/z: (ES$^+$) calcd ($C_{28}H_{49}NO_3$ + Na$^+$): 470.3605, found: 470.3606 (M + Na$^+$).

N,N-Bis(2-(prop-2-yn-1-yloxy)ethyl)oleamide 5d(O). Part 2: **4d** (15.4 g, 41.7 mmol), NaH 60% (3.67 g, 91.7 mmol), propargyl bromide (80% in toluene, 13.6 g, 91.7 mmol). A yellow oil (14.1 g, 76%); R_f = 0.3, 1 : 4 EtOAc : 40–60° pet. ether ν_{max}/cm^{-1} 3308 (≡C–H), 3003 (=C–H), 2922 (C–H), 2852 (C–H), 2115 (C≡C), 1639 (C=O), 1463 (C–H), 1442 (C–N), 1102 (C–O), 1031 (C–O), 755 (=C–H); ^{1}H NMR (500 MHz, CDCl$_3$) δ 5.47–5.27 (m, 2H, H^{9-10}), 4.14 (d, J = 2.0 Hz, 2H, H^C), 4.12 (d, J = 2.0 Hz, 2H, H^C), 3.72–3.63 (m, 4H, H^B), 3.63–3.53 (m, 4H, H^A), 2.45 (t, J = 2.0 Hz, 1H, H^E), 2.42 (t, J = 2.0 Hz, 1H, H^E), 2.36 (t, J = 7.5 Hz 2H, H^2), 2.02–1.99 (m, 4H, H^8, H^{11}), 1.67–1.58 (m, 2H, H^3), 1.31–1.27 (m, 20H, H^{4-7}, H^{12-17}), 0.88 (t, J = 7.0 Hz, 3H, H^{18}); ^{13}C NMR (126 MHz, CDCl$_3$) δ 173.74 (C=O), 129.95 (C=C), 129.82 (C=C), 79.67 (C^D), 79.32 (C^D), 74.83 (C^E), 74.47 (C^E), 68.72 (C^B), 68.04 (C^B), 58.49 (C^C), 58.27 (C^C), 48.79 (C^A), 46.39 (C^A), 33.09 (C^2), 31.92 (C^{16}), 29.86–29.02 (C^{chain}), 27.23 ($C^{8/11}$), 25.29 (C^3), 22.70 (C^{17}), 14.14 (C^{18}); m/z: (ES$^+$) calcd ($C_{28}H_{47}NO_3$ + Na$^+$): 468.3448, found: 468.3454 (M + Na$^+$).

(9Z,12Z)-N,N-Bis(2-(prop-2-yn-1-yloxy)ethyl)octadeca-9,12-dienamide 5e(L). Part 2: **4e** (22.4 g, 60.9 mmol), NaH 60% (5.4 g, 134.1 mmol), propargyl bromide (80% in toluene, 19.9 g, 134.1 mmol). A yellow oil (15.4 g, 57%); R_f = 0.3, 1 : 4 EtOAc : 40–60° pet. ether; ν_{max}/cm^{-1} 3305 (≡C–H), 3008 (=C–H), 2924 (C–H), 2853 (C–H), 1638 (C=O), 1464 (C–H), 1444 (C–N), 1102 (C–O), 1031 (C–O), 755 (=C–H); ^{1}H NMR (500 MHz, CDCl$_3$) δ 5.37–5.21 (m, 4H, H^{9-10}, H^{12-13}), 4.09 (d, J = 2.0 Hz, 2H, H^C), 4.06 (d, J = 2.0 Hz, 2H, H^C), 3.65–3.57 (m, 4H, H^B), 3.55–3.51 (m, 4H, H^A), 2.71 (t, J = 7.0 Hz, 2H, H^{11}), 2.40 (t, J = 2.0 Hz, 1H, H^E), 2.37 (t, J = 2.0 Hz, 1H, H^E), 2.31 (t, J = 7.5 Hz, 2H, H^2), 2.01–1.97 (m, 4H, H^8, H^{14}), 1.60–1.54 (m, 2H, H^3), 1.34–1.18 (m, 14H, H^{4-7}, H^{15-17}), 0.83 (t, J = 7.0 Hz, 3H, H^{18}); ^{13}C NMR (126 MHz, CDCl$_3$) δ 173.71 (C=O), 130.15 (C^{13}), 130.05 (C^{12}), 127.97 (C^{10}), 127.90 (C^{19}), 79.64 (C^D), 79.29 (C^D), 74.81 (C^E), 74.46 (C^E), 68.66 (C^B), 67.99 (C^B), 58.44 (C^C), 58.22 (C^C), 48.75 (C^A), 46.35 (C^A), 33.05 (C^2), 31.51 (C^{16}), 29.64 (C^7), 29.40 ($C^{15/4}$), 29.33 (C^5), 29.19 (C^6), 27.22 (C^{14}), 27.19 (C^8), 25.62 (C^{11}), 25.28 (C^3), 22.57 (C^{17}), 14.08 (C^{18}); m/z: (ES$^+$) calcd ($C_{28}H_{45}NO_3$ + Na$^+$): 466.3292, found: 466.3299 (M + Na$^+$).

(9Z,12Z,15Z)-N,N-Bis(2-(prop-2-yn-1-yloxy)ethyl)octadeca-9,12,15-trienamide 5f(Ln). Part 2: **4f** (5.5 g, 15.0 mmol), NaH (1.3 g, 33.1 mmol), propargyl bromide (80% in toluene, 4.9 g, 33.1 mmol). A pale-yellow oil (5.6 g, 84%); R_f = 0.3, 1 : 4 EtOAc : 40–60° pet. ether; ν_{max}/cm^{-1} 3296 (≡C–H), 3009 (=C–H), 2926 (C–H), 2854 (C–H), 2115 (C≡C), 1639 (C=O), 1463 (C–H), 1443 (C–N), 1100 (C–O), 1031 (C–O), 666 (=C–H); ^{1}H NMR (500 MHz, CDCl$_3$) δ 5.47–5.26 (m, 6H, H^{9-10}, H^{12-13}, H^{15-16}), 4.13 (d, J = 2.0 Hz, 2H, H^C), 4.11 (d, J = 2.0 Hz, 2H, H^C), 3.67 (t, J = 5.5 Hz, 2H, H^B), 3.63 (t, J = 5.5 Hz, 2H, H^B),

3.60–3.56 (m, 4H, H^A), 2.87–2.74 (m, 4H, H^{11}, H^{14}), 2.43 (t, J = 2.0 Hz, 1H, H^E), 2.40 (t, J = 2.0 Hz, 1H, H^E), 2.36 (t, J = 7.5 Hz, 2H, H^2), 2.08–2.02 (m, 4H, H^8, H^{17}), 1.76–1.45 (m, 2H, H^3), 1.39–1.22 (m, 8H, H^{4-7}), 0.96 (t, J = 7.5 Hz, 3H, H^{18}); ^{13}C NMR (101 MHz, CDCl$_3$) δ 175.85 (C=O), 132.07 (C=C), 130.44 (C=C), 128.39 (C=C), 128.38 (C=C), 127.80 (C=C), 127.24 (C=C), 79.77 (C^D), 79.42 (C^D), 74.89 (C^E), 74.53 (C^E), 68.83 (C^B), 68.13 (C^B), 58.60 (C^C), 58.38 (C^C), 48.88 (C^A), 46.48 (C^A), 33.20 (C^2), 29.75 (C^7), 29.53 ($C^{4/5}$), 29.32 (C^6), 27.35 (C^8), 25.73 (C^{11}), 25.64 (C^{14}), 25.41 (C^3), 20.66 (C^{17}), 14.40 (C^{18}); m/z: (ES$^+$) calcd ($C_{28}H_{43}NO_3$ + Na$^+$): 464.3135, found: 464.3145 (M + Na$^+$).

Polymer synthesis

General small scale thermal synthesis of polymers 6 and 7a–f, Fig. 3. To a solution of nitrile-N-oxide precursor **1a** (2.15 mmol in 2.15 mL of DMF) and dipolarophile **3, 5a–f** (1 eq., 2.15 mmol in 2.15 mL of DMF) was added molecular sieves (4 Å) and the mixture was stirred (50 rpm) at 25 °C for 30 min and then at 80 °C for 24 h. The reaction mixture was diluted with CHCl$_3$ (5 mL), filtered to remove the molecular sieves, the sieves were washed further with warm CHCl$_3$ (5 mL), the filtrate was then reduced *in vacuo* to leave the polymer in DMF. A small amount of CHCl$_3$ was added (2 mL) and the solution added dropwise to MeOH (40 mL). The precipitate was collected, washed with MeOH (3 × 25 mL), dissolved in CHCl$_3$ and the solvent removed *in vacuo* to give the polymers.

General large-scale base-mediated polymerisation using K$_2$CO$_3$ in EtOH. To a mixture of the stearate dialkyne **5c(S)**, (6 g, 13.4 mmol, 1.0 equiv.) and hydroximoyl dichloride **1a** or **1b** (3.12 g, 13.4 mmol, 1.0 eq.) in EtOH (50 mL) was added K$_2$CO$_3$ (4.0 g, 29.0 mmol, 2.0 eq.). After 24 h at room temperature water was added and the solution concentrated *in vacuo*. The crude mixture was extracted with CHCl$_3$ (2 × 50 mL), and the combined organic layers washed with water (2 × 50 mL), brine (50 mL) and dried over MgSO$_4$. The organic phase was removed under vacuum to provide the crude polymers.

Poly(1a-*co*-3). **1a** (500 mg, 2.15 mmol) and **3** (290 mg, 2.15 mmol) to give a pale orange/brown brittle solid (406 mg, 64%); ν_{max}/cm^{-1}: 3115 (C≡C–H), 2961 (C–H), 1651 (C=O), 1603 (C=O), 1406 (C–N), 901 (C–H); ^{1}H NMR (500 MHz,
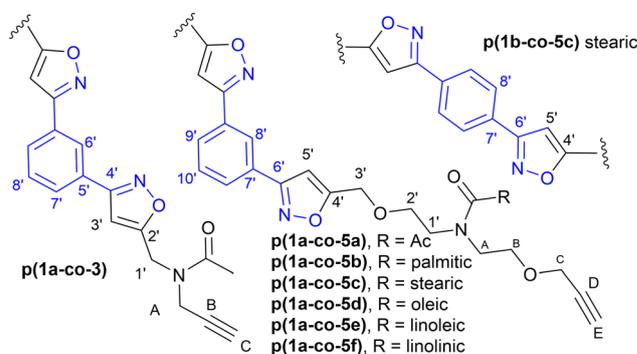

Fig. 3 Numbering system used in the NMR assignments in the Experimental section.

CDCl$_3$) δ 8.04 (brs, H$^{6'}$), 7.77 (brs, H$^{7'}$), 7.50 (brs, H$^{8'}$), 6.67–6.39 (brm, H$^{3'}$), 4.91–4.70 (brm, H$^{1'}$), 4.34 (brs, H^A-min), 4.18 (brs, H^A-maj), 2.36 (brs, H^B-maj), 2.27 (brs, H^B-min), 2.25 (s, CH$_3$); ^{13}C NMR (126 MHz, CDCl$_3$) δ 170.89 (C=O), 168.98 (C$^{2'}$), 168.06 (C$^{2'}$), 162.11 (C$^{4'}$), 129.78 (C$^{8'}$), 129.48 (C$^{5'}$), 129.17 (C$^{5'}$), 128.67 (C$^{7'}$), 128.38 (C$^{7'}$), 125.25 (C$^{6'}$), 125.21 (C$^{6'}$), 101.67 (C$^{3'}$), 101.46 (C$^{3'}$), 101.18 (C$^{3'}$), 100.93 (C$^{3'}$), 73.74 (C^C), 73.26 (C^C), 44.89 (C$^{1'}$), 43.39 (C$^{1'}$), 41.15 (C$^{1'}$), 40.83 (C$^{1'}$), 38.85 (C^A), 38.81 (C^A), 34.66 (C^A), 21.69 (C^{Me}), 21.59 (C^{Me}). (M_n = 4.4k, M_w = 6.5k, Đ = 1.5.)

Poly(1a-*co*-5a). **1a** (500 mg, 2.15 mmol) and **5a** (479 mg, 2.15 mmol) to give a pale orange/brown brittle solid (642 mg, 78%); ν_{max}/cm^{-1}: 2932 (C–H), 2870 (C–H), 1631 (C=O), 1613 (C=O), 1433 (C–N), 1099 (C–O), 908 (C–H); ^{1}H NMR (500 MHz, CDCl$_3$) δ 8.48 (s, minor signal for 3,4-isoxazole), 8.18 (brs, H$^{7'}$), 7.84 (brs, H$^{9'}$), 7.45 (brs, H$^{10'}$), 6.60 (brs, H$^{5'}$), 4.62 (brs, H$^{3'}$), 4.13 (d, J = 2.0 Hz, H^C), 4.11 (d, J = 2.0 Hz, H^C), 3.72 (brs, H$^{2'}$), 3.61 (brs, H$^{1'/A/B}$), 2.43 (t, J = 2.0 Hz, H^E), 2.41 (t, J = 2.0 Hz, H^E), 2.15 (brs, CH$_3$); ^{13}C NMR (126 MHz, CDCl$_3$) δ 171.97–171.45 (C=O), 169.89 (C$^{4'}$), 169.82 (C$^{4'}$), 161.96 (C$^{6'}$), 161.91 (C$^{6'}$), 129.80 (C$^{9'}$), 129.69 (C$^{7'}$), 128.45 (C$^{8'}$), 125.30 (C$^{10'}$), 101.45 (C$^{5'}$), 101.35 (C$^{5'}$), 75.05 (C^E), 74.72 (C^E), 69.88 (C$^{2'}$), 69.46 (C$^{2'}$), 68.85 (C^B), 75.05 (C^E), 74.72 (C^E), 69.88 (C$^{2'}$), 69.46 (C$^{2'}$), 68.85 (C^B), 68.05 (C^B), 64.21 (C$^{3'}$), 63.92 (C$^{3'}$), 58.62 (C^C), 58.44 (C^C), 50.34–49.82 (C$^{A/1'}$), 46.62 (C$^{A/1'}$), 46.43 (C$^{A/1'}$), 21.97 (C^{Me}). (M_n = 5.9k, M_w = 8.7k, Đ = 1.5.)

Poly(1a-*co*-5b(P)). **1a** (500 mg, 2.15 mmol) and palmitamide **5b(P)** (900 mg, 2.15 mmol) to give a malleable brown solid (1.08 g, 87%); ν_{max}/cm^{-1} 2921 (C–H), 2852 (C–H), 1636 (C=O), 1464 (C–H), 1437 (C–N), 1157 (C–O), 1102 (C–O), 912 (C–H); ^{1}H NMR (500 MHz, CDCl$_3$) δ 8.20 (brs, H$^{8'}$), 7.85 (brs, H$^{9'}$), 7.53–7.50 (m, H$^{10'}$), 6.65–6.54 (brm, H$^{5'}$), 4.76–4.52 (brm, H$^{3'}$), 4.13 (d, J = 2.0 Hz, H^C), 4.11 (d, J = 2.0 Hz, H^C), 3.78–3.54 (m, H$^{1'}$, H$^{2'}$, H^A, H^B), 2.43 (t, J = 2.0, H^E), 2.40 (t, J = 2.0, H^E), 2.39–2.30 (m, H^2), 1.65–1.51 (m, H^3), 1.33–1.13 (brm, H$^{4-15}$), 0.86 (brt, J = 6.5 Hz, H^{16}); ^{13}C NMR (126 MHz, CDCl$_3$) δ 173.97 (C^1), 169.93 (C$^{4'}$), 169.81 (C$^{4'}$), 161.93 (C$^{6'}$), 161.87 (C$^{6'}$), 129.82 (C$^{7'}$), 129.80–129.73 (C$^{10'}$), 129.71 (C$^{7'}$), 128.43 (C$^{9'}$), 125.32–125.18 (C$^{8'}$), 101.39–101.23 (C$^{5'}$), 79.74 (C^D), 79.38 (C^D), 74.99 (C^E), 74.62 (C^E), 70.04–69.83 (C$^{2'}$), 69.69–69.54 (C$^{2'}$), 68.91 (C^B), 68.21 (C^B), 64.35–64.14 (C$^{3'}$), 64.04–63.81 (C$^{3'}$), 58.60 (C^C), 58.41 (C^C), 49.23–48.81 (C$^{A/1'}$), 46.92–46.50 (C$^{A/1'}$), 33.44–33.19 (C^2), 32.03 (C^{14}), 29.99–29.17 (C$^{4-13}$), 25.42 (C^3), 22.80 (C^{15}), 14.24 (C^{16}). (M_n = 4.8k, M_w = 11.9k, Đ = 2.5.)

Poly(1a-*co*-5c(S)). **1a** (500 mg, 2.15 mmol) and stearamide **5c (S)** (961 mg, 2.15 mmol) to give a malleable brown solid (1.15 g, 88%); ν_{max}/cm^{-1}: 2921 (C–H), 2851 (C–H), 1637 (C=O), 1464 (C–H), 1438 (C–N), 1157 (C–O), 1102 (C–O), 913 (C–H); ^{1}H NMR (500 MHz, CDCl$_3$) δ 8.21 (brs, H$^{8'}$), 7.85 (brs, H$^{9'}$), 7.58–7.43 (m, H$^{10'}$), 6.66–6.54 (brm, H$^{5'}$), 4.67–4.56 (brm, H$^{3'}$), 4.13 (d, J = 2.0 Hz, H^C), 4.11 (d, J = 2.0 Hz, H^C), 3.77–3.56 (m, H$^{1'}$, H$^{2'}$, H^A, H^B), 2.43 (t, J = 2.0, H^E), 2.40 (t, J = 2.0, H^E), 2.39–2.32 (m, H^2), 1.66–1.54 (m, H^3), 1.36–1.08 (brm, H$^{4-17}$), 0.86 (brt, J = 6.5 Hz, H^{18}); ^{13}C NMR (126 MHz, CDCl$_3$) δ 173.98 (C^1), 169.94 (C$^{4'}$), 169.81 (C$^{4'}$), 161.93 (C$^{6'}$), 161.87 (C$^{6'}$), 129.82 (C$^{7'}$), 129.81–129.73 (C$^{10'}$), 129.72 (C$^{7'}$), 128.43 (C$^{9'}$),

125.34–125.19 (C$^{8'}$), 101.43–101.20 (C$^{5'}$), 79.74 (C^D), 79.39 (C^D), 74.99 (C^E), 74.62 (C^E), 70.04–69.86 (C$^{2'}$), 69.71–69.52 (C$^{2'}$), 68.92 (C^B), 68.21 (C^B), 64.32–64.14 (C$^{3'}$), 64.02–63.81 (C$^{3'}$), 58.61 (C^C), 58.41 (C^C), 49.19–48.90 (C$^{A/1'}$), 46.88–46.55 (C$^{A/1'}$), 33.42–33.18 (C^2), 32.04 (C^{16}), 29.92–29.32 (C$^{4-15}$), 25.42 (C^3), 22.81 (C^{17}), 14.25 (C^{18}). (M_n = 48k, M_w = 12.7k, Đ = 2.7.)

Poly(1a-*co*-5d(O)). **1a** (500 mg, 2.15 mmol) and oleamide **5d (O)** (956 mg, 2.15 mmol) to give a malleable brown solid (1.04 g, 80%); ν_{max}/cm^{-1}: 3002 (=C–H), 2923 (C–H), 2853 (C–H), 1637 (C=O), 1462 (C–H), 1438 (C–N), 1159 (C–O), 1102 (C–O), 912 (C–H); ^{1}H NMR (500 MHz, CDCl$_3$) δ 8.21 (brs, H$^{8'}$), 7.85 (brs, H$^{9'}$), 7.58–7.44 (brm, H$^{10'}$), 6.65–6.55 (brm, H$^{5'}$), 5.30 (brs, H$^{9/10}$), 4.71–4.52 (brm, H$^{3'}$), 4.49–4.44 (m, H^{CH_2}-min/cross-linked), 4.14 (brs, H^C), 4.10 (brs, H^C), 3.78–3.54 (m, H$^{1'}$, H$^{2'}$, H^A, H^B), 2.43 (brs, H^E), 2.40 (br, H^E), 2.39–2.30 (m, H^2), 2.03–1.90 (brm, H$^{9/11}$), 1.60 (brs, H^3), 1.25 (brs, H$^{4-7/12-17}$), 0.86 (brs, H^{18}); ^{13}C NMR (126 MHz, CDCl$_3$) δ 173.97 (C^1), 169.94 (C$^{4'}$), 169.81 (C$^{4'}$), 161.94 (C$^{6'}$), 161.88 (C$^{6'}$), 130.05 (C^{10}), 129.90 (C^9), 129.72 (C$^{7'}$), 129.83–129.74 (C$^{10'}$), 129.72 (C$^{7'}$), 128.45 (C^9), 125.35–125.16 (C$^{8'}$), 101.35 (C$^{5'}$), 75.02 (C^E), 74.66 (C^E), 70.06–69.81 (C$^{2'}$), 69.71–69.48 (C$^{2'}$), 68.91 (C^B), 68.20 (C^B), 64.32–64.08 (C$^{3'}$), 63.98–63.81 (C$^{3'}$), 58.61 (C^C), 58.42 (C^C), 49.19–48.87 (C$^{A/1'}$), 46.88–46.55 (C$^{A/1'}$), 33.37–33.19 (C^2), 32.02 (C^{16}), 29.96–29.12 (C$^{4-7/12-15}$), 27.39–27.27 (C^{11}), 25.41 (C^3), 22.80 (C^{17}), 14.25 (C^{18}). (M_n = 5.6k, M_w = 19.4k, Đ = 3.4.)

Poly(1a-*co*-5e(L)). **1a** (500 mg, 2.15 mmol) and linoleamide **5e(L)** (952 mg, 2.15 mmol) to give a malleable brown solid (984 mg, 76%); ν_{max}/cm^{-1}: 3276 (C≡C), 3007 (=C–H), 2925 (C–H), 2853 (C–H), 1636 (C=O), 1463 (C–H), 1437 (C–N), 1158 (C–O), 1101 (C–O), 912 (C–H); ^{1}H NMR (500 MHz, CDCl$_3$) δ 8.21 (brs, H$^{8'}$), 7.85 (brs, H$^{9'}$), 7.59–7.41 (brm, H$^{10'}$), 6.64–6.51 (brm, H$^{5'}$), 5.40–5.20 (brm, H$^{9/10/12/13}$), 4.68–4.56 (brm, H$^{3'}$), 4.49–4.44 (m, H^{CH_2}-min/crosslinked), 4.13 (brs, H^C), 4.11 (brs, H^C), 3.78–3.53 (m, H$^{1'}$, H$^{2'}$, H^A, H^B), 2.79–2.69 (brm, H^{11}), 2.51 (brs, H$^{cross-linked}$), 2.43 (brs, H^E), 2.40 (br, H^E), 2.39–2.29 (m, H^2), 2.07–1.95 (brm, H$^{8/14}$), 1.60 (brs, H^3), 1.27 (brs, H$^{4-7/15-17}$), 0.87 (brs, H^{18}); ^{13}C NMR (126 MHz, CDCl$_3$) δ 173.93 (C^1), 170.37–169.69 (C$^{4'}$), 162.04–161.84 (C$^{6'}$), 130.33 (C^{13}), 130.20 (C^9), 129.84–129.74 (C$^{10'}$), 129.71 (C$^{7'}$), 128.44 (C^9), 128.09 (C^{10}), 128.02 (C^{12}), 125.32–125.18 (C$^{8'}$), 101.33 (C$^{5'}$), 85.47 (C$^{cross-linked}$), 79.73 (C^D), 79.37 (C^D), 74.99 (C^E), 74.63 (C^E), 70.04–69.78 (C$^{2'}$), 69.73–69.49 (C$^{2'}$), 68.90 (C^B), 68.19 (C^B), 64.35–64.10 (C$^{3'}$), 64.02–63.80 (C$^{3'}$), 58.60 (C^C), 58.40 (C^C), 49.15–48.82 (C$^{A/1'}$), 46.86–46.48 (C$^{A/1'}$), 33.37–33.09 (C^2), 31.61 (C^{16}), 29.88–29.18 (C$^{4-7/15}$), 27.35–27.27 (C$^{8/14}$), 25.73 (C^{11}), 25.38 (C^3), 22.68 (C^{17}), 14.19 (C^{18}). (M_n = 6.3k, M_w = 33.6k, Đ = 5.3.)

Poly(1a-*co*-5f(Ln)). **1a** (500 mg, 2.15 mmol) and linoleamide **5f(Ln)** (948 mg, 2.15 mmol) to give a malleable brown solid (917 mg, 71%); ν_{max}/cm^{-1}: 3269 (C≡C), 3008 (=C–H), 2925 (C–H), 2854 (C–H), 1635 (C=O), 1461 (C–H), 1438 (C–N), 1159 (C–O), 1101 (C–O), 912 (C–H); ^{1}H NMR (500 MHz, CDCl$_3$) δ 8.21 (brs, H$^{8'}$), 7.85 (brs, H$^{9'}$), 7.58–7.42 (brm, H$^{10'}$), 6.67–6.53 (brm, H$^{5'}$), 5.43–5.23 (brm, H$^{9/10/12/13/15/16}$), 4.73–4.50 (brm, H$^{3'}$), 4.50–4.45 (m, H^{CH_2}-min/cross-linked), 4.13 (brs, H^C), 4.11 (brs, H^C), 3.72–3.52 (brm, H$^{1'}$, H$^{2'}$, H^A, H^B), 2.78 (brs, H$^{11/14}$),

2.57 (brs, H$^{cross-linked}$), 2.43 (brs, H^E), 2.40 (br, H^E), 2.39–2.25 (m, H^2), 2.08–1.95 (brm, H$^{8/17}$), 1.60 (brs, H^3), 1.37–1.16 (brm, H$^{4-7}$), 0.96 (brs, H^{18}); ^{13}C NMR (126 MHz, CDCl$_3$) δ 173.95 (C^1), 170.27–169.70 (C^4), 162.09–161.76 (C^6), 132.09 (C$^{9/10/12/13/15/16}$), 130.44 (C$^{9/10/12/13/15/16}$), 129.85–129.75 (C$^{10'}$), 128.55–128.43 (C^9), 128.41 (C$^{9/10/12/13/15/16}$), 128.39 (C$^{9/10/12/13/15/16}$), 127.83–127.75 (C$^{9/10/12/13/15/16}$), 127.24 (C$^{9/10/12/13/15/16}$), 125.33–125.17 (C^8), 101.34 (C$^{5'}$), 85.39 (C$^{cross-linked}$), 79.74 (C^D), 79.39 (C^D), 75.04 (C^E), 74.66 (C^E), 70.04–69.79 (C$^{2'}$), 69.66–69.47 (C$^{2'}$), 68.91 (C^B), 68.21 (C^B), 64.34–64.13 (C^3), 64.02–63.80 (C^3), 58.62 (C^C), 58.42 (C^C), 49.18–48.83 (C$^{A/1'}$), 46.90–46.54 (C$^{A/1'}$), 33.38–33.17 (C^2), 29.87–29.20 (C$^{4-7}$), 27.35 (C^8), 25.74 (C^{11}), 25.65 (C^{14}), 25.40 (C^3), 20.68 (C^{17}), 14.42 (C^{18}). (M_n = 4.3k, M_w = 16.5k, $Đ$ = 3.9.)

Poly(1b-co-5c(S)). **1b** (3.12 g, 13.4 mmol), stearamide **5c(S)** (6.0 g, 13.4 mmol), K$_2$CO$_3$ (4.0 g, 29.0 mmol, 2.0 eq.) in EtOH (50 mL) to give a pale-yellow solid (7.33 g, 90%); ν_{max}/cm^{-1}: 2916 (C–H), 2849 (C–H), 1638 (C=O), 1592 (C=N), 1573 (C=N), 1101 (C–O); ^{1}H NMR (500 MHz, CDCl$_3$) δ 7.85 (s, H$^{8'}$), 6.56–6.52 (m, H$^{5'}$), 4.63 (d, J = 2.0 Hz, H^3), 4.12 (d, J = 2.0 Hz, H^C), 3.67 (m, H$^{1'}$, H$^{2'}$, H^A, H^B), 2.42–2.40 (m, H^E), 2.36–2.30 (m, H^2), 1.63–1.52 (m, H^3), 1.34–1.03 (m, H$^{4-17}$), 4.12 (brt, J = 6.8 Hz, H^{18}); ^{13}C NMR (126 MHz, CDCl$_3$) δ 173.86 (C^1), 169.79 (C^4), 169.69 (C^4), 161.71 (C^1), 161.65 (C^6), 130.79 (C^7), 127.34 (C^8), 101.17 (C$^{5'}$), 101.08 (C$^{5'}$), 79.67 (C^E), 79.27 (C^E), 74.86 (C^D), 74.49 (C^D), 69.81 (C$^{2'}$), 69.51 (C$^{2'}$), 68.72 (C^B), 68.04 (C^B), 64.10 (C^3), 63.77 (C^3), 58.49 (C^C), 58.27 (C^C), 48.94 (C$^{1'/A}$), 48.77 (C$^{1'/A}$), 46.62 (C$^{1'/A}$), 46.37 (C$^{1'/A}$), 33.19 (C^2), 31.92 (C^{16}), 29.71 (C$^{4-15}$), 29.67 (C$^{4-15}$), 29.57 (C$^{4-15}$), 29.51 (C$^{4-15}$), 29.37 (C$^{4-15}$), 25.31 (C^3), 22.69 (C^{17}), 14.13 (C^{18}); (M_n = 4.9k, M_w = 25.3k, $Đ$ = 5.9).

Results and discussion

Isoxazole polymers are normally prepared by the reaction of ester or ether derived alkyne monomers and aromatic derived nitrile-N-oxides, (*e.g.*, derived from thermal elimination of HCl from **1a–b**).[8] Few examples of reactions with amide derived alkyne monomers have been reported. Due to restricted rotation around the amide bond the analysis, structure determination and conformational space of the products is often not straightforward. A further issue is that conventional polystyrene or PMMA standards in GPC analysis can lead to inaccurate measures of molecular weights. Consequently, our initial investigations focused on the polymerization of the non-bioderived model propargyl amide **3** and propargyl ether **5a** where the potential fatty acid chain was replaced with a methyl group to facilitate analysis. Monomer **3** was prepared in 93% yield from the acetylation of dipropargyl amine with acetic anhydride at 100 °C, while the propargyl ether **5a** was prepared in 44% yield by NaH deprotonation of the known diol[21] **4a** at −78 °C followed by reaction with two equivalents of propargyl bromide at room temperature, Fig. 2. As expected, both compounds exhibited two sets of sharp signals for the two inequivalent alkyne groups in both the ^{1}H 500 MHz and

^{13}C 126 MHz NMR. Variable temperature analysis (^{1}H) of **5a** indicated a barrier to rotation around the amide bond, of ΔG = 75.7 ± 1.3 kJ mol^{-1} which is identical to that reported for **4a** (75.7 kJ mol^{-1}).[21]

Polyisoxazole formation has mainly been undertaken using thermal polymerisation between 80–100 °C and so thermal analysis (TGA) of both monomers (heating at 10 °C min^{-1} from 25–600 °C under N$_2$) was undertaken to determine if they exhibited suitable stability for further reactions (**3**, $T_{5\%}$ = 133 °C, $T_{20\%}$ = 170 °C, **5a**, $T_{5\%}$ = 240 °C, $T_{20\%}$ = 285 °C where $T_{5\%}$ and $T_{20\%}$ are the temperature for 5% and 20% mass loss respectively), see ESI.† Although the less flexible monomer **3** showed lower stability, both were suitable for further study. Reacting an appropriate excess of either **3** or **5a** (dipolarophile, monomer A) with nitrile-N-oxide precursor **1a** (monomer B) using the procedure of Takata[8] (80 °C, DMF, 4 Å MS, 24 h) produced authentic small oligomer samples of (AB)$_1$A type (*e.g.* O^1**3** = (**3–1a–3**), O^1**5a** = (**5a–1a–5a**)) and (AB)$_2$A type (O^2**3** = (**3–1a–3–1a–3**), O^2**5a** = (**5a–1a–5a–1a–5a**)) with alkyne end groups for ^{1}H NMR and GPC analysis, Fig. 4a. In addition, a 1 : 1 stoichiometry of **3** or **5a** with **1a** under the same reaction conditions was used to prepare the polymers **p(1a-co-3)** and **p(1a-co-5a)** respectively. After precipitation from MeOH the crude polymers were further washed with MeOH to remove the lower molecular weight materials. Initial analysis of the ^{1}H NMR of the reactions of the propargyl ether **5a** indicates that the major mode of cycloaddition proceeds to give the expected 3,5-isoxazole product, Fig. 4b, although traces (<5%) of the alternative 3,4-regioisomer (8.49 ppm and 4.50 ppm) were detected, Fig. 4d. Relative integration of the H$^{3'}$ signals adjacent to the isoxazole moiety with the H^C signals of the end group allowed information on the degree of polymerisation to be determined, (**p(1a-co-3)** DP = 16, **p(1a-co-5a)** DP = 10). For the oligomer O^1**5a** at room temperature, the ^{1}H NMR spectrum showed two singlets for the acetyl group (0.55 : 0.45), while four distinct singlet chemical environments were observed for the isoxazole H$^{5'}$ proton, indicating a relatively complicated conformational analysis for such a simple molecule, Fig. 4c.

Restricted rotation around the two amides, as well as the C–C aryl-isoxazole bonds of the *meta* substituted aromatic ring needs to be considered, Fig. 4a. Variable temperature ^{1}H NMR of O^1**5a** in d$_6$-DMSO provided an estimated ΔG barrier to rotation around the amide functionality of 75.1 ± 1.3 kJ mol^{-1}, (T_c = 343 K), which is similar to that observed in the monomer. The four environments for the isoxazole protons reduced to two at elevated temperature but coalescence was not observed at 373 K. Interestingly, the more compact oligomer O^1**3** (based upon the reaction of 2 equivalents of **3** with **1a**) exhibited a lower barrier to rotation of ΔG = 72.1 ± 1.3 kJ mol^{-1}.

The GPC results for the reactions of propargyl ether **5a** are shown in Fig. 5a. Authentic samples of the monomer **5a** and the two (AB)$_n$A type oligomers O^1**5a** (ABA) and O^2**5a** ((AB)$_2$A) were used as references to confirm polymerisation. GPC data for both polymers confirmed that washing the crude polymers with MeOH (**p'(1a-co-5a)**) facilitated removal of lower molecular weight oligomers and unreacted starting materials, Fig. 5a.
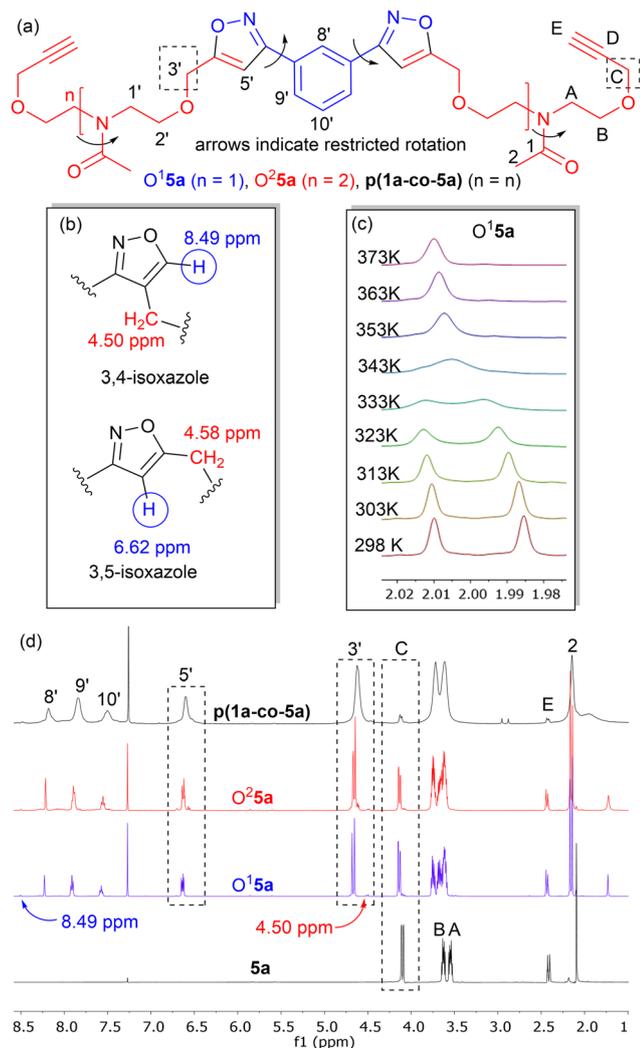
Fig. 4 (a) Structures of oligomers, O^{1}5a and O^{2}5a, and polymer **p(1a-co-5a)** with the numbering system used in this paper; (b) the 500 MHz ^{1}H NMR values for 3,4- and 3.5-isoxazoles in O^{1}5a; (c) the 500 MHz ^{1}H variable temperature NMR of oligomer O^{1}5a between 298–373 K showing T_c = 343 K; (d) stacked plot of 500 MHz ^{1}H NMR spectrum of monomer **5a**, the two oligomers O^{1}5a and O^{2}5a, and the polymer **p(1a-co-5a)** showing (i) minor amounts of 3,4-isoxazole at 8.49 ppm and 4.50 ppm, (ii) the position of signals representative of polymer chains (3′) and end groups (C) with the relative integration providing the degree of polymerisation, (iii) the positions and assignments of key signals.

Fig. 5 (a) GPC in DMF of propargyl ether monomer **5a**, oligomers O^{1}5a and O^{2}5a, MeOH wash of **p(1a-co-5a)** and polymer **p(1a-co-5a)**; (b) MALDT-TOF-MS of **P6** between 900–3000 Da using DCTB as matrix showing a repeat unit of 295 Da for two species (AB)$_n$A and (AB)$_n$ type.

Trace amounts of lower molecular weight species were detected in the GPC of the polymers themselves. **p(1a-co-5a)**, M_n = 5.9k, M_w = 8.7k, $Đ$ = 1.5, repeat unit = 383 Da, **p(1a-co-3)**, M_n = 4.4k, M_w = 6.5k, $Đ$ = 1.5, repeat unit = 295 Da.

Insight into the nature of the linkages present in the polymers was investigated using MALDI-TOF-MS which indicated several species with the correct repeating unit for both polymers. The MALDI-TOF-MS for **p(1a-co-3)** is shown as an example and shows the expected linear alkyne terminated (AB)$_n$A series (monomer A = alkyne **3** and monomer B = nitrile-*N*-oxide derived from **1a**, the linear polymer is terminated with an alkyne end group). No termination of the polymer with an
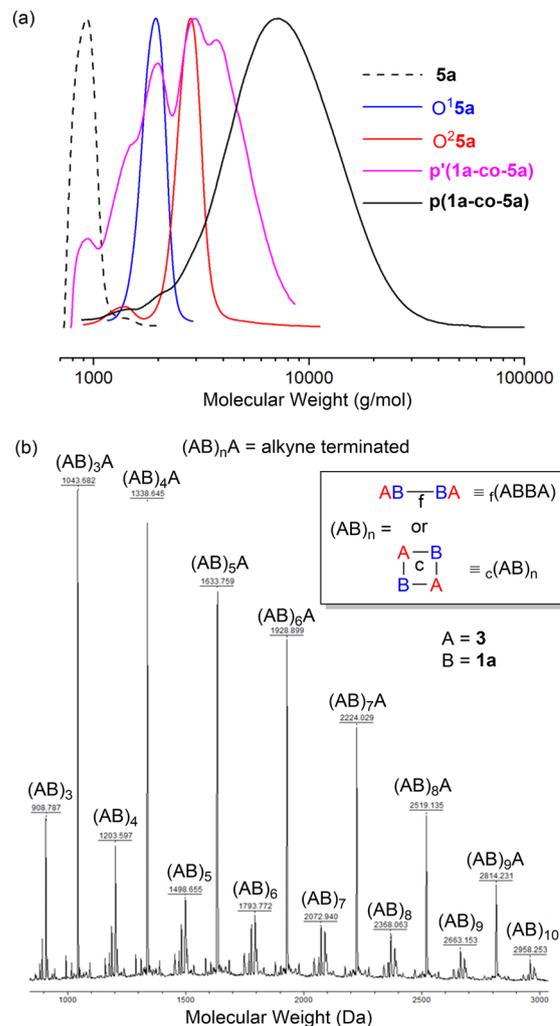
oximoyl chloride (C=N(OH)Cl) end group was detected, indicating HCl elimination must be complete under the reaction conditions. One series was assigned as (AB)$_n$ type polymers. This is unlikely to be an ABAB type oligomer terminated with one end group of an alkyne (monomer A) and the other a nitrile-*N*-oxide (monomer B). While this is the norm for step-growth polymerisation, the nitrile-*N*-oxide itself is not normally a stable functional group at elevated temperature instead undergoing dimerization to give either 1,4,2,5-dioxa-diazines or furoxans.[22] A few poorly stable nitrile-*N*-oxides are known at room temperature, but they are restricted to inherently sterically encumbered cases (*e.g.* 4-substituted-2,6-di-methylbenzonitrile oxide).[23,24] It is very unlikely that the polymers contain nitrile-*N*-oxide end groups due to the high temperature of the reaction and the lack of an intense peak in the IR spectrum at around 2200–2300 cm^{-1}. Consequently, the (AB)$_n$ type polymers may be tentatively assigned as either (a) a cyclic species, $_c$(AB)$_n$, with no end groups, or (b) a species

where any growing chain nitrile-*N*-oxide undergoes dimerization to give a furoxan of type **2**, f(ABBA)$_n$, with alkyne end groups, Fig. 5b. No characteristic signals of aryl furoxans were detected in the infrared spectrum of either **p(1a-*co*-3)** or **p(1a-*co*-5a)**, (namely the characteristic peaks at 1590 cm^{-1}, 1572 cm^{-1} and 1503 cm^{-1}), suggestive that the (AB)$_n$ species are cyclic in nature, for infrared spectra of polymers see ESI.†

Both polymers **p(1a-*co*-3)** and **p(1a-*co*-5a)** exhibited similar thermal stability: **p(1a-*co*-3)** ($T_{5\%}$ = 251 °C, $T_{20\%}$ = 349 °C), and **p(1a-*co*-5a)** ($T_{5\%}$ = 249 °C, $T_{20\%}$ = 339 °C). These values were significantly higher than those of their respective monomers: **p(1a-*co*-3)** ($T_{5\%}$ = +116 °C, $T_{20\%}$ = +179 °C), and **p(1a-*co*-5a)** ($T_{5\%}$ = +9 °C, $T_{20\%}$ = +54 °C). As expected, the more flexible polymer **p(1a-*co*-5a)** exhibited a lower glass transition temperature (T_g = 51.0 °C) compared to **p(1a-*co*-3)** (T_g = 112.0 °C). Given that the primary focus of this work was to prepare biobased polyisoxazoles with lower T_g's than vanillin derived materials[11] (ranging from 60–80 °C), our next step concentrated on incorporating fatty acid derivatives using the more flexible ethanolamine derived chains.

Biobased polymers from fatty amides

Polymerisation of the saturated monomers derived from palmitic **5b(P)** and stearic **5c(S)** acids were expected to behave similarly to **5a**. However, the unsaturated analogues based upon oleic **5d(O)**, linoleic **5e(L)** and linolenic **5f(Ln)** acids have the potential to undergo cross-linking/branching to form isoxazolines *via* addition to the differing levels of unsaturation present in their chains, Fig. 6. However, it was expected that the competing reaction to give the isoxazolines would be relatively slow due to the internal nature of the alkene groups compared to the terminal alkynes.[25] To quantify how likely this was and to obtain spectroscopic information to help determine the level of cross-linking/branching in subsequent soluble polymers, we reacted methyl oleate **6** with phenyloximoyl chloride **7** under the same polymerisation conditions as
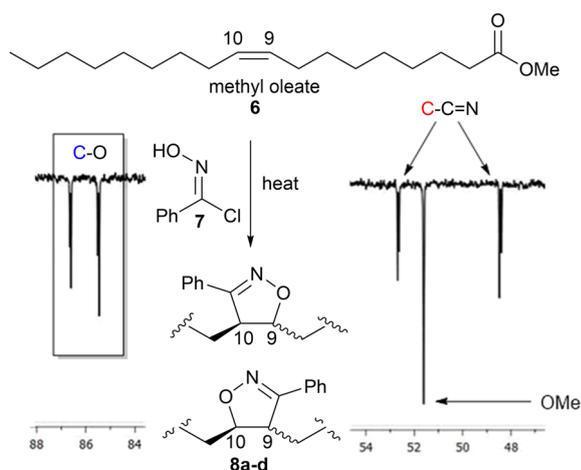
the model studies. The reaction produced four compounds **8a–d**, two regioisomers in equal amounts, with each regioisomer consisting of two diastereomers in a roughly 1 : 1 ratio (based upon the ^{1}H NMR) in very low yield (8%) after 24 hours. While the formation of two regioisomers was expected due to the limited regiospecific driving force between the nitrile-*N*-oxide and the internal alkene[26] the formation of diastereomers was not expected due to the stereospecific nature of the cycloaddition. The low yield, after an extended reaction time at elevated temperature, indicated that while isoxazoline formation was possible under these conditions it was not particularly fast. It is also possible that the extended reaction time allowed the generated HCl to mediate an epimerisation of the acidic proton adjacent to the imine group in **8a–d** or that reversible HCl addition to the unreacted methyl oleate alkene in **6** allowed equilibration of the dienophile stereochemistry.

The position of the characteristic ^{1}H NMR signals for the CH protons next to the oxygen atom and one diastereomer next to the nitrogen atom of the isoxazoline group **8a–d** resonated in areas that would make them inappropriate as reference handles due to overlap with polymer resonances. On the other hand, the positions of the C^9 and C^{10} carbon signals in the ^{13}C NMR spectrum for each compound were characteristic (86.6, 85.4, 52.6, 48.4 ppm) and appeared in spectral regions expected to be clear in the linear polymers (based upon the model studies **p(1a-*co*-3)** and **p(1a-*co*-5a)**), Fig. 6.

Reaction of each of the fatty acid derived monomers **5b–f** with 1.0 equivalent of **1a** at 80 °C in DMF for 24 h with 4 Å molecular sieves produced the corresponding polymeric materials, Table 1. Interestingly, as the level of unsaturation in the fatty acid side chains increased, the degree of polymerisation (as determined by ^{1}H NMR spectra) of the materials reduced, Fig. 7. Tentative traces of branching were confirmed through the ^{13}C spectrum of the soluble materials, presumably due to the slower rate of addition to the disubstituted alkene group compared to the terminal alkyne groups. The yields of the materials also

Fig. 6 Portion of the 126 MHz ^{13}C spectrum of **8a–d** on CDCl$_3$ showing the characteristic isoxazoline signals at 86.6, 85.4, 52.6 and 48.4 ppm.

Table 1 Thermal and molecular weight data for the polymers **1a-*co*-3**, **1a-*co*-(5a–f)**

Polymer	Yield (%)	DP^a	T_g^b (°C)	$T_{5\%}^c$ (°C)	M_n^d (kDa)	M_w^d (kDa)	Đ
1a-*co*-3	64	16	112	249	4.4	6.5	1.5
1a-*co*-5a	78	10	51.0	251	5.9	8.7	1.5
1a-*co*-5b(P) palmitic	87	9	5.7	272	4.8	11.9	2.5
1a-*co*-5c(S) stearic	84	10	4.8	279	4.8	12.7	2.7
1a-*co*-5d(O) oleic	80	6	−1.1	255	5.6	19.4	3.4
1a-*co*-5e(L) linoleic	76	5	3.2	253	6.3	33.6	5.3
1a-*co*-5f(Ln) linolenic	71	3	6.1	247	4.3	16.5	3.9

^{a} Determined from ^{1}H NMR by integration of the peaks at 4.63 ppm (peak 3′, in the polymer) and 4.12 ppm (peak C, CH$_2$ of the end group in polymer), see Fig. 7. ^{b} Determined from DSC, heat rate 10 °C min^{-1}. ^{c} Temperature of 5% decomposition from TGA, heat rate 10 °C min^{-1}. ^{d} Determined from GPC, eluent CHCl$_3$.
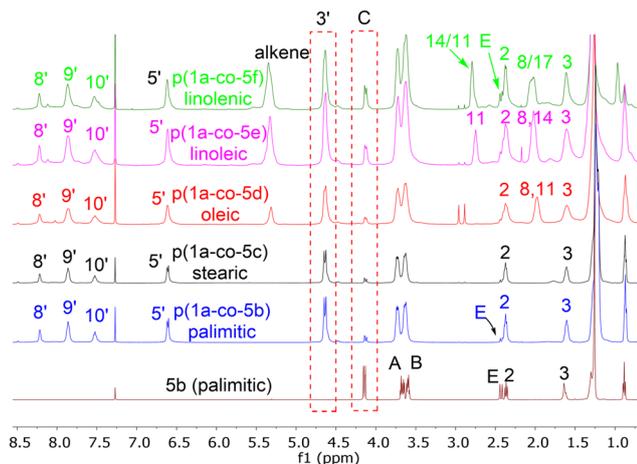
Fig. 7 Stacked plot of 500 MHz ^{1}H NMR of fatty acid derived polymers **p(1a-*co*-(5a–f))** and palmitic monomer **5b(P)** showing increasing levels of unreacted alkyne end groups as evidenced by peaks 'C' and 'E' relative to polymer chains.

Fig. 8 (a) Normalised GPC data for the stearate monomer **5c** and ABA type oligomer O^1 **5c** and fatty acid derived polymers **p(1a-*co*-(5b–f))** showing wider molar mass dispersity for unsaturated oleic **p(1a-*co*-5d (O))**, linoleic **p(1a-*co*-5e(L))**, and linolenic **p(1a-*co*-5f(Ln))** derivatives; (b) T_g values for **p(1a-*co*-3)** and fatty acid derived polymers **p(1a-*co*-(5b–f))** from differential scanning calorimetry (DSC), heat rate 10 °C min^{-1}.

dropped with the level of unsaturation, due to increased levels of unreacted monomers but not significantly.

It was possible to isolate a pure sample of the stearate ABA oligomer O^1 **5c(S)** to serve as a reference for GPC and for VT ^{1}H NMR analysis, ($\Delta G_{rotation}$ = 75.2 ± 1.3 kJ mol^{-1}), Fig. 8a. The normalised GPC data shows a relatively wide molar mass dispersion (*Đ*) for the unsaturated polymers: oleic **p(1a-*co*-5d(O))** *Đ* = 3.4, linoleic **p(1a-*co*-5e(L))** *Đ* = 5.3 and linolenic **p(1a-*co*-5f (Ln))** *Đ* = 3.9. These values are higher than expected for a typical step growth polymerisation and are most likely attributed to branching due to competing isoxazoline formation by reaction with the internal alkene groups, although more complex processes such as competing cyclic formation or furoxan formation, or a mixture of all three cannot be ruled out.

Thermal analysis of the fatty acid derived polymers **p(1a-*co*-(5b–f))** indicated significantly lower T_g values (−1.1 °C to 6.1 °C) compared to **p(1a-*co*-5a)** as expected, (Fig. 8b), due to the incorporation of the flexible C16–C18 chains. Assuming no branching occurred during the polymerisation the expected order of T_g values should be linolenic **p(1a-*co*-5f(Ln))** < linoleic **p(1a-*co*-5e(L))** < oleic **p(1a-*co*-5d(O))** < stearic **p(1a-*co*-5c(S))** < palmitic **p(1a-*co*-5b(P))** < **p(1a-*co*-5a)** < **p(1a-*co*-3)**. The fact that the linolenic **p(1a-*co*-5f(Ln))** and linoleic **p(1a-*co*-5e(L))** materials have marginally higher T_g values than the oleic **p(1a-*co*-5d(O))** material suggests that branching is occurring in these polyunsaturated derivatives. Additionally, all the bio-based polymers show degraded thermal stability compared to the stearate ABA type oligomer O^1 **5c(S)**. While the polyunsaturated linolenic **p(1a-*co*-5f(Ln))** and linoleic **p(1a-*co*-5e(L))** materials exhibit initially lower thermal stability ($T_{5\%}$) below 300 °C and slightly higher stability above 300 °C than the saturated analogues, the inherent complication of branching discouraged us from any further investigation, Fig. 9.

MALDI-TOF-MS of the stearate polymer **p(1a-*co*-5c(S))**, Fig. 10, indicated the presence of two repeating species with a
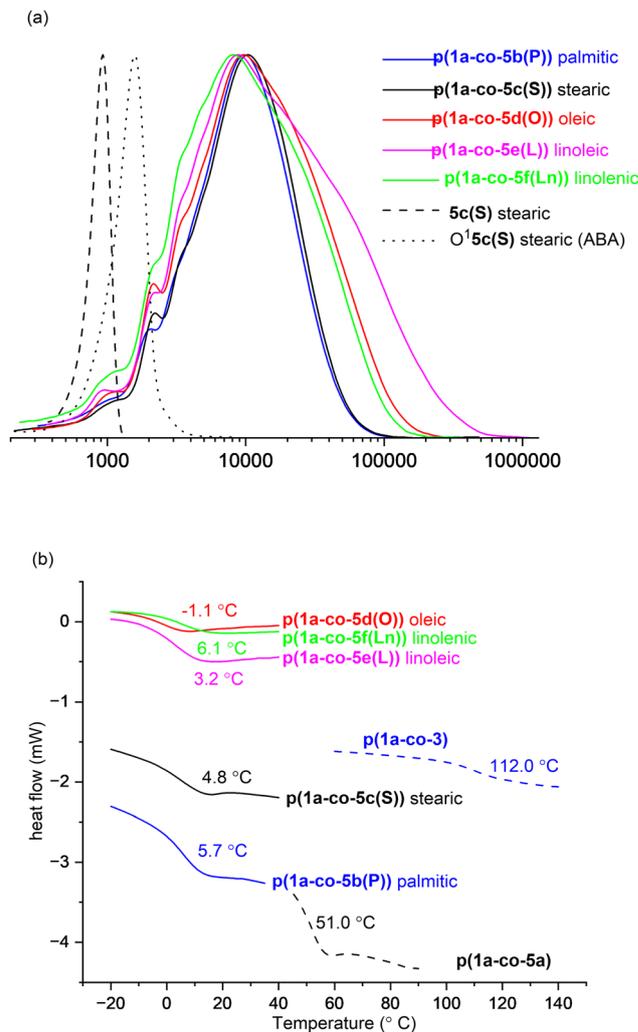
repeating unit of 607 Da. These species represent linear (AB)$_n$A type polymers terminated by alkyne end groups (1684, 2291, 2896, 3505 Da respectively) and additionally (AB)$_{2-4}$ type species tentatively assigned as cyclic $_c$(AB)$_n$ materials. The alternative linear structure (AB)$_n$ terminated with one alkyne and one nitrile oxide end group was discounted due to the instability of the nitrile oxide under the reaction conditions and its propensity to dimerise *via* furoxan formation although it can't be completely ruled out. The alternative linear furoxan (f) linked material $_f$(AB-BA)$_n$ with two alkyne end groups was also discounted due to the absence of evidence of furoxan formation in the infrared spectrum. Although the infrared spectrum of the fatty acid derived polymers **p(1a-*co*-(5b-f))** did not indicate furoxan formation, it would be more energy efficient to be able to undertake the polymerisation at ambient temperatures. This approach could help suppress any competing
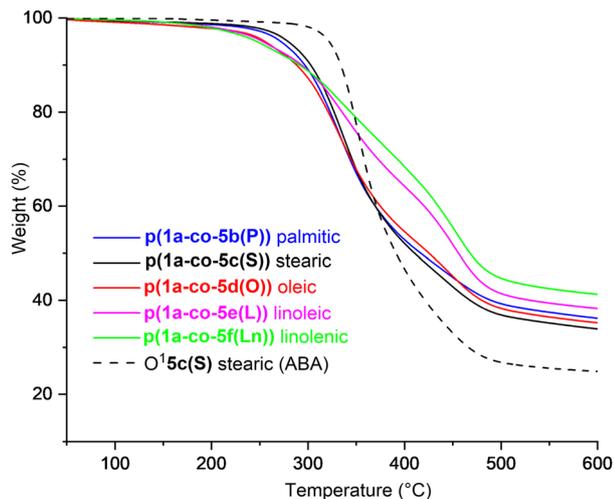
Fig. 9 Thermal gravimetric analysis plots from 50–600 °C for fatty acid derived polymers **p(1a-*co*-(5b–f))**, compared to the stearate ABA type oligomer O[1] **5c**, heat rate 10 °C min⁻¹.
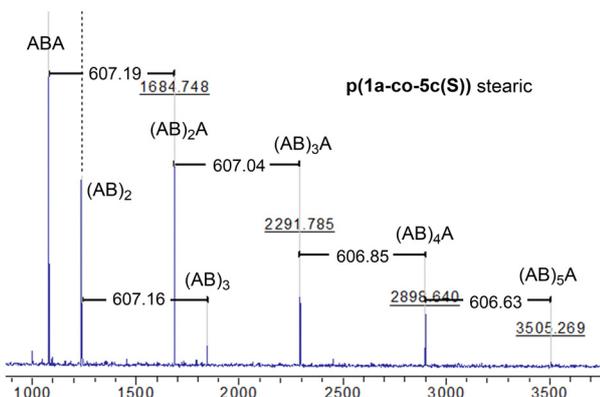

Fig. 10 MALDI-TOF-MS of stearate **p(1a-*co*-5c(S))** showing two polymeric species (the (AB)$_n$A type and the (AB)$_n$ type, both with a repeat unit of 607 Da).

Fig. 11 (a) 500 MHz ¹H NMR spectra of stearate derived **p$_{base}$(1a-*co*-5c (S))** and **p$_{base}$(1b-*co*-5c(S))** showing high number of repeat units and tentative assignment of cyclic oligomers; (b) GPC in CHCl₃ of **p$_{base}$(1a-*co*-5c(S))** and **p$_{base}$(1b-*co*-5c(S))** showing area tentatively assigned as cyclic oligomers.

side reactions that might affect the efficiency of the polymerisation and consequently lower molecular weights. We briefly explored differing base-mediated polymerisation conditions using the stearate derived monomer **5c(S)** as a test substrate. While organic bases such as triethylamine have been used to facilitate nitrile oxide formation from oximoyl chloride **4a** at elevated temperatures,[27] we found that inorganic bases, specifically K₂CO₃, were the most efficient for mediating the reaction at room temperature in our experiments. A summary of the different conditions investigated, including added copper salts and different bases, NaHCO₃, Na₂CO₃, and K₂CO₃ in various solvents (DCM, DMF, acetone, THF, diethyl ether, ethanol) can be found in the ESI.† The best conditions involved utilising K₂CO₃ in the renewable solvent ethanol, which furnished a material with the highest observed molecular weight (M_n = 19.0k, M_w = 36.2k, Đ = 1.9), [**5c** and **1a**, K₂CO₃, EtOH], Fig. 11b, but with a bimodal molar mass distribution. Scaling up of the test reactions from 150 mg to 6.0 g of
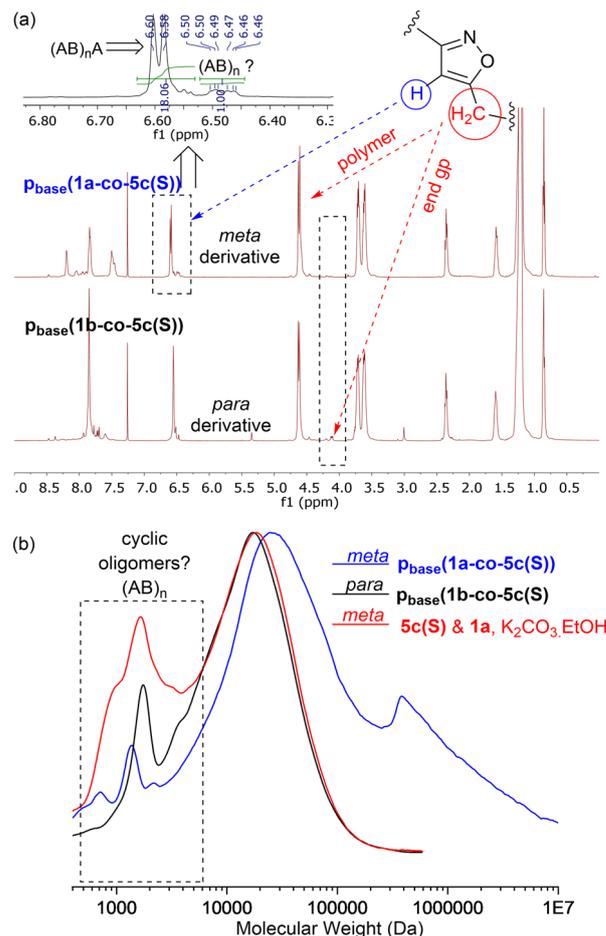
stearate monomer **5c(S)** utilising 1 equivalent of either **1a** or **1b** with K₂CO₃ in ethanol over 24 hours resulted in the formation of the base mediated *meta* linked stearate derived polymer **p$_{base}$(1a-*co*-5c(S))** as a sticky pale solid and the corresponding *para* derived material **p$_{base}$(1b-*co*-5c(S))** as a white solid in yields of 88% and 90% respectively. Both materials completely dissolved in CHCl₃ and THF and both exhibited large dispersity in their GPC traces in these solvents indicative of secondary processes to the desired step growth polymerisation occurring. Indeed, the low molar mass tailing in both GPC traces could be indicative of an inactive species, tentatively assigned as the cyclic (AB)$_n$ species which can no longer propagate [**p$_{base}$(1b-*co*-5c(S))** (M_n = 4.9k, M_w = 25.3k, Đ = 5.9), **p$_{base}$(1a-*co*-5c(S))** (M_n = 11.4k, M_w = 88.4k, Đ = 25.8), Fig. 11b]. The *meta* derived material **p$_{base}$(1a-*co*-5c(S))** did not exhibit any observable signals in the ¹H NMR at 4.12 ppm for the end group –CH₂– protons of the propargyl group, confirming high molecular weights, while trace evidence of alkyne terminated end groups in the ¹H NMR of **p$_{base}$(1b-*co*-5c(S))** was observed indicating a DP of 21, Fig. 11a.

Further evidence that the low molar mass species observed from the GPC data were cyclic in nature came from the MALDI-TOF-MS, Fig. 12b. Both materials showed two peaks at 1237 Da and 1845 Da for stearate derived $(AB)_2$ and $(AB)_3$ oligomers. No higher homologues were detected in the MS range (0–5000 Da) suggesting these species were inactive cyclic homologues which cannot propagate further, Fig. 12a. If these low molar mass $(AB)_n$ type oligomers were not cyclic in nature, but instead were the alternative linear furoxan linked materials of the type $_f(AB–BA)$ with alkyne end groups, these linear chains would continue to grow and would have reacted further to give higher homologues which were not detected. This allows us to tentatively speculate that the minor peaks in the range of 6.50–6.46 ppm in the ^1H NMR of $\mathbf{p_{base}(1a\text{-}co\text{-}5c(S))}$, can be assigned to $H^{5'}$ isoxazole proton in these cyclic materials.

In both polymers, traces of a species at 1397 Da were observed which must contain at least one furoxan linkage, most likely in the cyclic material of type $_c(ABBAB)$. Indeed, analysis of the infrared spectrum of the stearate derived $\mathbf{p_{base}(1a\text{-}co\text{-}5c(S))}$ indicated a shoulder on the main C≡N stretch peaks at 1592 cm^{-1} indicative of furoxan formation. If furoxan formation is detected within the cyclic oligomer it is also statistically likely that it is incorporated into the growing linear polymer chains in a second polymerisation process. This unde-

sired secondary polymerisation process could be the origin of the broader molar mass distribution (1×10^5–1×10^7 Da) observed for $\mathbf{p_{base}(1a\text{-}co\text{-}5c(S))}$, Fig. 11b. If K$_2CO_3$ mediated polymerisation does in fact produces a polyisoxazole with random incorporation of furoxan linkages it might be expected to have different thermal properties. Thermal analysis indicated the polymers produced via the room temperature base-mediated approach were significantly more thermally stable than those derived from heating in DMF alone. This is presumably due to the significantly larger molecular weights and/or furoxan incorporation, [stearate derived $\mathbf{p(1a\text{-}co\text{-}5c(S))}$ $T_{5\%}$ = 279 °C vs. $\mathbf{p_{base}(1a\text{-}co\text{-}5c(S))}$ $T_{5\%}$ = 339 °C (+60 °C), $\mathbf{p_{base}(1a\text{-}co\text{-}5c(S))}$ $T_{5\%}$ = 328 °C (+49 °C)]. In addition, both polymers exhibited higher T_g values than the smaller molecular weight polymer $\mathbf{p(1a\text{-}co\text{-}5c(S))}$ prepared thermally. The DSC of both polymers indicated melting points (T_m = 31 °C for $\mathbf{p_{base}(1a\text{-}co\text{-}5c(S))}$), and ($T_m$ = 48 °C for $\mathbf{p_{base}(1b\text{-}co\text{-}5c(S))}$), and DMA analysis provided T_g's of 31 °C and 62 °C respectively. The higher value for para derived $\mathbf{p_{base}(1b\text{-}co\text{-}5c(S))}$ is presumably due to the linear nature of the linking nitrile oxide influencing packing and chain mobility of the polymer ends, with the linear chains packing more efficiently than those derived from the meta $\mathbf{p_{base}(1a\text{-}co\text{-}5c(S))}$. Although nitrile-$N$-oxides are known to react with nucleophiles to give hydroxamic acids,[28,29] no evidence of this reaction manifold incorporating ethoxide (from K$_2$CO$_3$ and EtOH) was detected.

Conclusions

Biobased polyisoxazoles derived from thermal polymerisation of both saturated and unsaturated C16–C18 fatty acid derived alkynes **5b–f** with **1a** exhibit lower T_g's, but similar thermal stability compared to those derived from acetate materials **3** and **5a**. While the degree of polymerisation determined by ^1H NMR drops as the level of unsaturation in the fatty chains increases: palmitic derivative $\mathbf{p(1a\text{-}co\text{-}5b(P))}$ ~ stearic derivative $\mathbf{p(1a\text{-}co\text{-}5c(S))}$ > oleic derivative $\mathbf{p(1a\text{-}co\text{-}5d(O))}$ > linoleic derivative $\mathbf{p(1a\text{-}co\text{-}5e(L))}$ > linolenic derivative $\mathbf{p(1a\text{-}co\text{-}5f(Ln))}$, the M_n, M_w and dispersity increases for the unsaturated derivatives. This increase is due to competitive isoxazoline formation resulting from the competing reaction with the internal alkene groups with **1a** in the unsaturated derivatives, which (a) introduces branching within the growing polymer chains and (b) changes the stoichiometry of the desired reacting functional groups. Although evidence of branching could not be confirmed in the ^1H NMR spectra, very weak signals around 86 ppm and 48 ppm in the ^{13}C spectra of the oleic $\mathbf{p(1a\text{-}co\text{-}5b(O))}$, linolenic $\mathbf{p(1a\text{-}co\text{-}5b(L))}$, and linoleic $\mathbf{p(1a\text{-}co\text{-}5b(Ln))}$ derived polymers confirmed this process, as did GPC data. Normally T_g would decrease as the level of unsaturation in the side chains increased, as they are more kinked, reducing the ability to pack, this is observed in the series: palmitic derivative $\mathbf{p(1a\text{-}co\text{-}5b(P))}$ > stearic derivative $\mathbf{p(1a\text{-}co\text{-}5c(S))}$ > oleic derivative $\mathbf{p(1a\text{-}co\text{-}5d(O))}$. However, the T_g increases marginally from the oleic derivative $\mathbf{p(1a\text{-}co\text{-}5d(O))}$ < the linoleic derivative
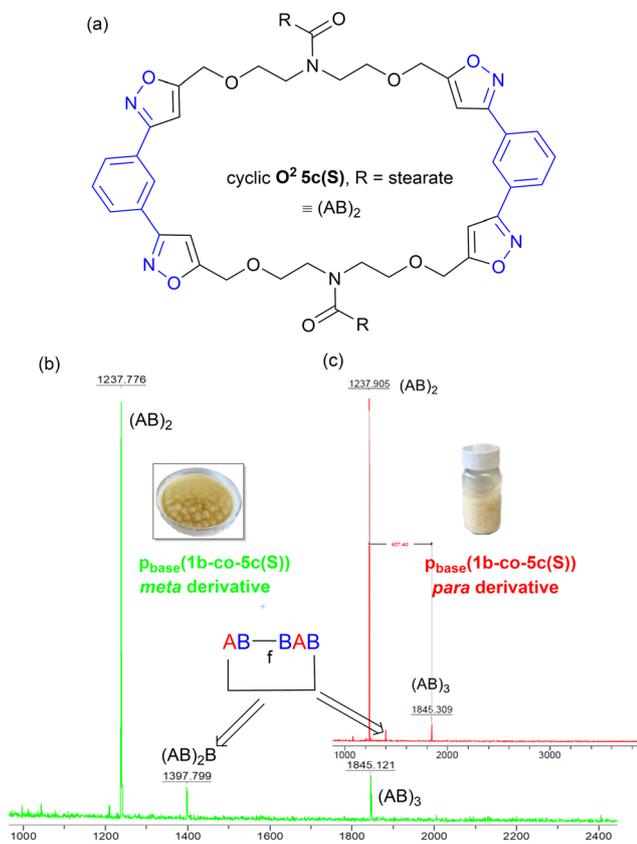

Fig. 12 (a) Postulated structure of the stearate derived $(AB)_2$ species O^2 **5c**, (b) the MALDI-TOF-MS spectrum of meta $\mathbf{p_{base}(1a\text{-}co\text{-}5c(S))}$, and (c) the MALDI-TOF-MS spectrum of para $\mathbf{p_{base}(1b\text{-}co\text{-}5c(S))}$.

p(1a-co-5e(L)) < the linolenic derivative p(1a-co-5f(Ln)), presumably caused by the greater opportunities for branching.

Conducting the polymerisation of stearate monomer 5c(S) with either the *meta* 1a or *para* 1b nitrile-*N*-oxide precursors under basic conditions (K_2CO_3, EtOH) led to polymers with higher molecular weights and $Đ$'s and higher T_g values, although GPC indicated a small oligomeric distribution followed by the main polymeric distribution. MALDI-TOF-MS of all the polymers indicated the expected repeat units for linear $(AB)_nA$ type polymers (with terminal alkyne end groups) as well as a $(AB)_n$ species which could be cyclic in nature (lacking end groups) or incorporate a furoxan linkage. However, while there was little evidence of competing furoxan formation for polymers produced thermally as observed in both the MALDI-TOF-MS or the infrared spectra, (p(1a-co-3) and p(1a-co-(5a–f))), there was some evidence for furoxan incorporation in polymers p_{base}(1a-co-5c(S)) and p_{base}(1b-co-5c(S)) prepared using the base-mediated process.

In general, the T_g values from the biobased materials in this study (−1.1 °C to 62.0 °C) complement those derived from biobased vanillin derivatives (60–80 °C).[11] This suggests a broad spectrum of thermal properties can be achieved with biobased materials, making them versatile for various potential applications.

Author contributions

AJC was the principal investigator responsible for the conceptualisation, project administration, supervision and original draft writing. NOSJ prepared polymers p(1a-co-3) and p(1a-co-(5a–f)) using thermal conditions and undertook the investigation, helped develop the methodology, undertook formal analysis and reviewed the writing, AA undertook polymerisation tests at room temperature and prepared polymers p_{base}(1a-co-5c(S)) and p_{base}(1b-co-5c(S)) and undertook the investigation, helped develop the methodology, undertook formal analysis and reviewed and edited the writing.

Conflicts of interest

There are no conflicts to declare.

Acknowledgements

Notes and references

1 V. V. Rostovtsev, L. G. Green, V. V. Fokin and K. B. Sharpless, *Angew. Chem., Int. Ed.*, 2002, **41**, 2596.

2 Z. Geng, J. J. Shin, Y. Xi and C. J. Hawker, *J. Polym. Sci.*, 2021, **59**, 963.

3 G. Delaittre, N. K. Guimard and C. Barner-Kowollik, *Acc. Chem. Res.*, 2015, **48**, 1296.

4 E. Coutouli-Argyropoulou, P. Lianis, M. Mitakou, A. Giannoulis and J. Nowak, *Tetrahedron*, 2006, **62**, 1494.

5 C. G. Overberger and S. Fujimoto, *J. Polym. Sci., Part B: Polym. Lett.*, 1965, **3**, 735.

6 Y. Iwakura, S. Shiraishi, M. Akiyama and M. Yuyama, *Bull. Chem. Soc. Jpn.*, 1968, **41**, 1648.

7 Y. Iwakura, K. Uno, S.-J. Hong and H. A. Tatsuhiko, *Polym. J.*, 1971, **2**, 36.

8 Y. Koyama, M. Yonekawa and T. Takata, *Chem. Lett.*, 2008, **37**, 918.

9 Y.-G. Lee, Y. Koyama, M. Yonekawa and T. Takata, *Macromolecules*, 2009, **42**, 7709.

10 Y.-G. Lee, M. Yonekawa, Y. Koyama and T. Takata, *Chem. Lett.*, 2010, **39**, 420.

11 J. J. Q. Mah, C.-G. Wang, N. Surat'man, S. F. D. Solco, A. Suwardi, S. Wang, X. J. Loh and L. Zibiao, *ACS Appl. Polym. Mater.*, 2023, **5**, 6757.

12 T. Pasinszki, B. Hajgató, B. Havasi and N. P. C. Westwood, *Phys. Chem. Chem. Phys.*, 2009, **11**, 5263.

13 U. Biermann, U. T. Bornscheuer, I. Feussner, M. A. R. Meier and J. O. Metzger, *Angew. Chem., Int. Ed.*, 2021, **60**, 20144.

14 U. Biermann, U. T. Bornscheuer, M. A. R. Meier, J. O. Metzger and H. J. Schäfer, *Angew. Chem., Int. Ed.*, 2011, **50**, 3854.

15 J. Hong, Q. Luo and B. K. Shah, *Biomacromolecules*, 2010, **11**, 2960.

16 J. Hong, Q. Luo, X. Wan, Z. S. Petrović and B. K. Shah, *Biomacromolecules*, 2012, **13**, 261.

17 M. C. Floros, A. L. Leão and S. S. Narine, *BioMed Res. Int.*, 2014, **2014**, DOI: 10.1155/2014/792901.

18 D. R. Kelly, S. C. Baker, D. S. King, D. S. deSilva, G. Lord and J. P. Taylor, *Org. Biomol. Chem.*, 2008, **6**, 877.

19 L. P. Guan, X. Sui, X. Q. Deng, D. H. Zhao, Y. L. Qu and Z. S. Quan, *Med. Chem. Res.*, 2011, **20**, 601.

20 S. M. Sagnella, C. E. Conn, I. Krodkiewska and C. J. Drummond, *Phys. Chem. Chem. Phys.*, 2011, **13**, 13370.

21 R. A. Aitken, M. H. Smith and H. S. Wilson, *J. Mol. Struct.*, 2016, **1113**, 151.

22 F. DeSarlo, *J. Chem. Soc., Perkin Trans. 1*, 1974, 1951.

23 M. Shiro, M. Yamakawa, T. Kubota and H. Koyama, *Chem. Commun.*, 1968, 1409.

24 M. M. Krayushkin, L. G. Vorontsova, M. G. Kurella and M. A. Kalik, *Russ. Chem. Bull.*, 1993, **42**, 689.

25 J. Plumet, *ChemPlusChem*, 2020, **85**, 2252.

26 R. Huisgen, *Angew. Chem., Int. Ed. Engl.*, 1963, **2**, 633.

27 P. Carmella, A. Corsaro, A. Compagnini and F. Marinone Albini, *Tetrahedron Lett.*, 1983, **24**, 4377.

28 N. Masina, Y. E. Choonara, P. Kumar, L. C. du Toit, M. Govender, S. Indermun and V. A. Pillay, *Carbohydr. Polym.*, 2017, **157**, 1226.

29 M. Volanti, D. Cespi, F. Passarini, E. Neri, F. Cavani, P. Mizsey and D. Fozer, *Green Chem.*, 2019, **21**, 885.